Narrowing of Topological Bands due to Electronic Orbital Degrees Freedom

Jörn W. F. Venderbos, Maria Daghofer, and Jeroen van den Brink
Institute for Theoretical Solid State Physics, IFW Dresden, 01171 Dresden, Germany
(Received 22 June 2011; published 8 September 2011)

The fractional quantum Hall effect has been predicted to occur in the absence of magnetic fields and at high temperature in lattice systems that have flat bands with a nonzero Chern number. We demonstrate that orbital degrees of freedom in frustrated lattice systems lead to a narrowing of topologically nontrivial bands. This robust effect does not rely on fine-tuned long-range hopping parameters and is directly relevant to a wide class of transition-metal compounds.

DOI: 10.1103/PhysRevLett.107.116401 PACS numbers: 71.10.−w, 71.27.+a, 73.43.Cd

Investigating the repercussions of topology on the electronic states in condensed matter systems has a long and rich history. The integer quantum Hall (IQH) effect, discovered [1] in 1980, was soon understood to be a profound manifestation of the topological properties of the Landau levels. The quantized Hall conductance was shown to be a topological invariant that classifies the ground state [2]. Later that decade, Haldane [3] showed that the IQH state is not restricted to two-dimensional (2D) electron gases in a strong magnetic field. It can also be realized in lattice systems without Landau levels, by introducing electrons on a lattice with complex hoppings that break time-reversal symmetry. In recent years, topologically nontrivial electronic phases were moreover discovered in time-reversal invariant insulators [4–7], leading to the quantum spin Hall effect in two dimensions [8,9] and to the existence of protected 2D Dirac fermions on the surface of 3D topological insulators [10,11] and a related quantum Hall effect [12].

These presently much studied 2D and 3D topological insulators are time-reversal invariant lattice systems that can therefore be perceived as a further generalization of the quantum Hall states. The generalization of fractional quantum Hall (FQH) states, the fractional counterpart of the IQH states, was considered only very recently [13–15]. Such a lattice FQH effect will be quite different from the ordinary FQH in 2D electron gases, for instance requiring a variational wavefunction distinct from the Laughlin wave function [16,17], and it can occur without magnetic field and potentially at high temperature [13–15]. Its realization in a material system would offer an exciting prospect for quantum computation, since the presence of non-Abelian FQH states allows for the creation of topologically protected qbits [18]. Creating the analogue of the FQH effect in a lattice system requires the fractional filling of topologically nontrivial bands, which should be very narrow [13–15], so that the electron-electron interactions can dominate over the kinetic energy and induce FQH states [19].

The theoretical approach used to progress toward this goal so far relies on the fine-tuning of the electron kinetic energy in model Hamiltonians containing bands with the correct topological properties [13–15,20]. Such a flattening procedure of the bands usually requires tuning (very) long-range hopping parameters to a set of quite peculiar strengths, which in real materials represents a rather formidable challenge from an experimental point of view.

We consider orbital degrees of freedom as an alternative agent for band flattening. Orbitals naturally occur in many transition-metal (TM) compounds, which at the same time feature strong electron-electron interactions [21,22]. We concentrate on manganites, where Mn^{3+} ions are in a high-spin $3d^4$ configuration, with three electrons in the more localized t_{2g} states forming a spin of $3/2$ and one electron in either of the two more itinerant e_g orbitals ferromagnetically coupled to this spin. Apart from other $3d$ systems besides Mn, the versatile class of TM oxides also contains $4d$ and $5d$ materials with orbital degrees of freedom, of which ruthenates [23] and iridates [24,25] are important examples.

We will show that in the presence of a chiral spin texture, such an orbital makeup leads to nearly flat topologically nontrivial bands. It is well established that geometric frustration may stabilize noncoplanar spin-chiral magnetic textures when itinerant electrons couple to localized spins [26–30]. The Berry phase acquired by the electrons then leads to topologically nontrivial bands [27,28,31–33]. The pronounced spatial anisotropy of the e_g and t_{2g} orbitals strongly affects the symmetry of hopping integrals, even suppressing hopping completely along some directions [21]. This can result in very flat bands like the dispersionless bands found in several multiorbital TM compounds – a number of antiferromagnetic phases in cubic manganites are stabilized by such a mechanism [34,35]. Here, we report a strong orbital-induced flattening of topological bands in spin-chiral phases on frustrated kagome and triangular lattices, demonstrating that orbital degrees of freedom of transition-metal ions generically provide a route to realizing a lattice version of the FQH effect. We also present indications that residual interactions can then induce a FQH state.

Chiral spin textures.—We first summarize the situation on the triangular and kagome lattices for mobile charge carriers without orbital degrees of freedom in presence of a nontrivial spin-texture. The Kondo Lattice Model, which describes the interaction between localized (t_{2g}) spins and itinerant (e_g) electrons, exhibits a topologically nontrivial chiral spin state on the triangular lattice [27–29]. This state has a four-sublattice ordering, illustrated in Fig. 1(a) and a finite scalar spin chirality $\langle \mathbf{S}_1 \cdot \mathbf{S}_2 \times \mathbf{S}_3 \rangle \neq 0$ for spins on the corners of triangles. The situation then becomes equivalent to electrons hopping on a triangular lattice with a fictitious gauge flux of $\phi = \pi/2$ threading each triangle; see Fig. 1. The effective electronic Hamiltonian has a two-site unit cell [27] and two bands, with Chern numbers ± 1, separated by a gap. On the kagome lattice, a staggered flux pattern, shown in Fig. 1, can result from topologically nontrivial spin states, where a flux ϕ threads each triangle and a flux -2ϕ each hexagon [31]. Time-reversal symmetry is broken for $\phi \neq 0$, π and two gaps open, leading to three bands. The middle band has zero Chern number, but the lowest and highest are topologically nontrivial with $C = \mp\mathrm{sgn}(\sin\phi)$ [31]. However, all topologically nontrivial bands have a considerable dispersion on both lattices, which we will now show to be substantially reduced by the presence of an orbital degree of freedom.

Orbital degree of freedom—In many TM oxides, the TM ions are inside oxygen octahedra, which are edge-sharing

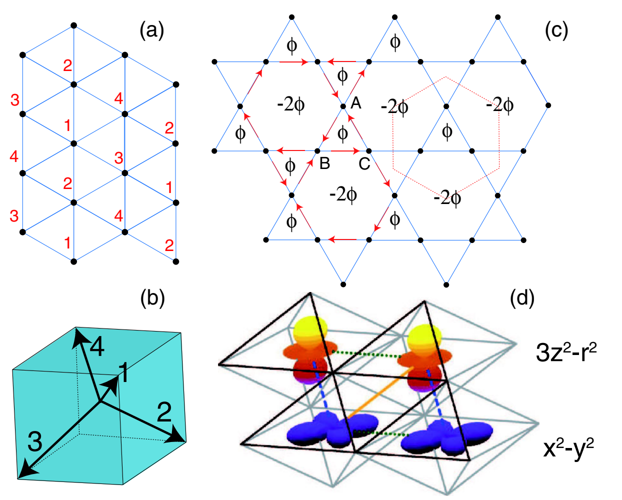

FIG. 1 (color online). (a) Chiral spin ordering on the triangular lattice. (b) Spins forming a regular tetrahedron, numbers refer to sites in (a). (c) Flux-phase state on the kagome lattice. The unit cell is indicated by the dashed hexagon and the gauge choice by arrows; a flux ϕ threads each triangle. (d) Nearest-neighbor hopping geometry in lattices with triangular symmetry. Grey lines illustrate the oxygen octahedra, black front facets illustrate the triangular geometry. Thick dotted, dashed, and solid lines indicate the bonds corresponding to the hopping matrices $\hat{T}_1$, $\hat{T}_2$, and $\hat{T}_3$. Two $d_{3z^2-r^2}$ (top) and $d_{x^2-y^2}$ (bottom) orbitals are also shown.

in a triangular lattice; see Fig. 1. The cubic symmetry splits the TM d levels into three t_{2g} and two e_g orbitals. We focus mainly on the latter, but later also demonstrate an analogous effect for the former. Along the $\mathbf{a}_1 = (0, 1)$ direction, indicated by a dotted line in Fig. 1, hopping for e_g orbitals conserves orbital flavor and is given by t (t') for the $|x^2 - y^2\rangle$ ($|3z^2 - r^2\rangle$) orbital. Hoppings along the other two bonds are obtained by a rotation in orbital space, the hopping matrices along all three bonds are given by Eq. (1) in [36]. We use t as unit of energy and vary the material-dependent ratio t'/t between -1 and 1, concentrating on $t'/t < 0$ inferred from direct overlaps of the orbitals [37]. For our fillings of approximately one electron per site, the Jahn-Teller effect is important and can induce a uniform crystal field $H_{\mathrm{JT}} = \Delta(n_x - n_z)$, lifting orbital degeneracy [38].

The two sites of the unit cell in the spin-chiral phase [27] together with the two e_g orbitals give a 4×4 Hamiltonian in momentum space; see [36]. Figure 2 shows the energy bands calculated for a strip geometry, with periodic boundary conditions in one direction and two edges in the orthogonal direction. For a large enough crystal-field splitting $\Delta > t$, t', a gap separates bands with different orbital character. Within each subsystem, chiral magnetic order induces a further splitting into two topologically nontrivial bands with Chern numbers $C = \pm 1$. This is unambiguously indicated by the topological edge states connecting the bands with $C > 0$ and $C < 0$ in Fig. 2(a). The transverse Hall conductivity σ^n_{xy} is shown in Fig. 2(b) and directly reflects the topological character of the bands.

The gap between the topological bands is smaller in the upper $(x^2 - y^2)$ sector, but robust between the two $3z^2 - r^2$ bands below the crystal-field gap. The upper band of the $3z^2 - r^2$ sector with $C = -1$, has a weak dispersion, becoming nearly flat for $t' \approx -t/2$, see Fig. 2(a). The figure of merit quantifying the flatness is the ratio of the gaps M separating it from other bands to its band width W. Here we monitor both the "topological" gap (M_+), which is induced by chiral order and the "trivial" crystal-field gap (M_{-1}), which separates it from the $x^2 - y^2$ sector above. Figure 3(a) shows these ratios depending on t' and Δ, the relevant figure of merit is the smaller of the two ratios M_+/W and M_{-1}/W. It is appreciable in a broad range of Δ and t', reaching a maximum of $\sim$4.25 for $\Delta = 2.5$ and $t' = -0.45$.

We can also consider t_{2g} orbitals $|xy\rangle$, $|xz\rangle$, and $|yz\rangle$. The hopping matrices are given in Eq. (2) of [36] and consist of interorbital hopping t (primarily via ligand oxygen ions [39]) and orbital-conserving hopping t' due to direct overlap [40]. In a threefold symmetry, the t_{2g} manifold is further split into one a_{1g} and two e'_g states separated by a crystal-field H_{JT} [41]. Qualitatively, we find similar behavior as for e_g orbitals, but the figure of merit reaches $M/W \approx 14$, see Fig. 3(b). This extraordinarily large M/W reflects the very large spatial anisotropy of t_{2g}

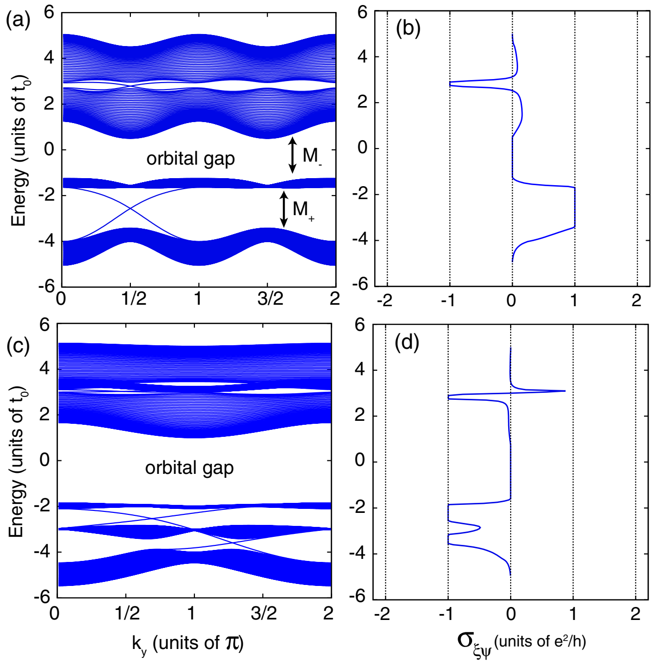

FIG. 2 (color online). Top: kagome lattice, bottom: triangular lattice. Left: bands of a strip geometry, clearly showing the chiral edge states of the flattened bands. Right: off-diagonal Hall conductivity as function of chemical potential, providing the Chern numbers for the flat bands. For the Kagome lattice $t' = -0.46$, $\Delta = 2.75$, $\phi = \pi/4$ and for the triangular case $t' = -0.46$, $\Delta = 2.5$.

hopping integrals, well-known in triangular vanadates [39] and cobaltates [40].

After discussing the triangular lattice, we now come to e_g orbitals on the kagome lattice illustrated in Fig. 1(b). The lattice has a three-site unit cell, and one proceeds with an approach analogous to the two-site unite cell discussed above, for details see [36]. Bands are again separated by the crystal field into two parts with a different orbital character; see Fig. 2. While the $x^2 - y^2$ sector is hardly gapped, the $3z^2 - r^3$ sector shows three subbands with $C = 0, \pm 1$ similar to the one-band model [31]. Again, the topological character can be inferred from edge states and is confirmed by the Hall conductivity shown in Fig. 2(d) and as for the triangular lattice, the top band of the $3z^2 - r^3$ sector (with $C = +1$) is very flat for $t' \approx -t/2$. The figure of merit M/W is plotted in Fig. 3(c); it reaches values up to ~ 3.5 for $\Delta = 2.75$ and $t' = -0.45$, compared to $W/M \lesssim 1$ in the one-band model without orbital degrees of freedom.

FQH state induced by residual interactions.—After showing that orbital degrees of freedom can lead to flat bands with Chern number $C \neq 0$, we analyze the impact of Coulomb repulsion on the triangular lattice e_g system. We include electron-electron interactions

$$H_{\rm int} = U \sum_i n_{i,x^2-y^2} n_{i,3z^2-r^2} + V \sum_{\langle i,j \rangle, \alpha\beta} n_{i,\alpha} n_{j,\beta}, \qquad (1)$$

where $n_{i,\alpha}$ is the electron density in orbital α on site i, U acts on electrons occupying two orbitals on the same site, and V gives the nearest-neighbor (NN) interaction. Following Refs. [15,19], we use exact diagonalization (ED) to study signatures of FQH-like states for a filling $1/3$ of the topologically nontrivial flat band. For details on the parameters and the method, see [36]. We find an approximate threefold ground-state manifold, which is an indication for the topological degeneracy of a FQH state. The three "ground states" cross each other upon inserting a magnetic flux[42], see Fig. 4 and [36], in agreement with results for other models [15,43,44].

Discussion—The flattening due to the orbital degrees of freedom presented here can be further enhanced by introducing and fine-tuning longer-range hopping integrals, as in one-band models. Perfectly flat and topologically nontrivial bands ($M/W \to \infty$) can in principle be obtained by allowing for arbitrarily long-range hoppings [14]. We do not explore this here, as we aim to show that the anisotropy inherent in d-orbital degrees of freedom can robustly

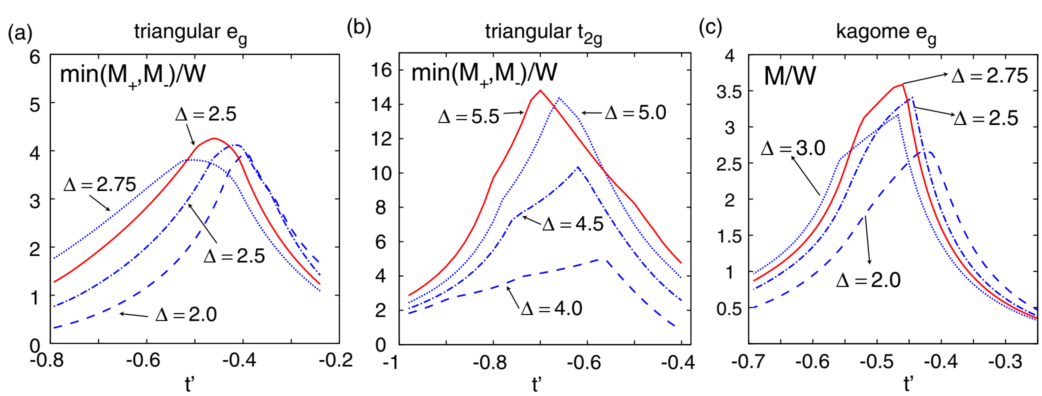

FIG. 3 (color online). (a) The smallest band gap over bandwidth ratios for e_g electrons the triangular lattice, for the gaps M_+ and M_- indicated in Fig. 2(a). (b) The same for t_{2g} electrons on a triangular lattice and (c) for e_g on the kagome lattice. Orbital splittings are indicated by Δ.

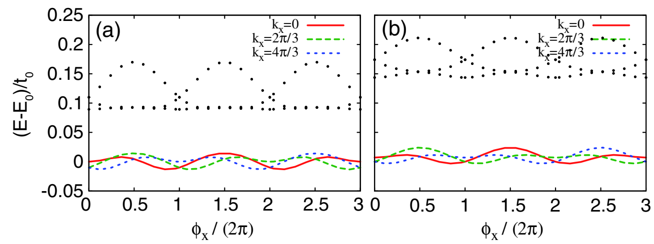

FIG. 4 (color online). Lowest energies of the interacting e_g system on the triangular-lattice, depending on flux inserted for (a) $U = 2$, $V = 1$, and (b) $U = 4$, $V = 2$. The ED results presented here were obtained for a 2×6 system with $t'/t = -0.46$ and $\Delta = 1.5$; see [36].

flatten topological bands even with purely NN hopping, and obtain flattening ratios up to $M/W \approx 4$ ($M/W \approx 14$) for e_g (t_{2g}) systems.

Orbital degrees of freedom are directly relevant to numerous well-known TM systems. Manganese compounds alone, which closely correspond to the e_g model studied here, occur in a variety of crystal structures: in simple cubic or square lattices in $La_{1-x}Sr_xMnO_3$ and $LaSrMnO_4$, honeycomb in, e.g., Li_2MnO_3 or $(Bi_3Mn_4O_{12})NO_3$ but also in strongly frustrated pyrochlore lattices as in, e.g., $Ti_2Mn_2O_7$ and in triangular lattices as in $YMnO_3$. The pyrochlore lattice, in particular, is realized by the B-site TM ions in the very common spinel crystal structure, and can be thought of as consisting of kagome and triangular layers stacked along the (1,1,1) direction. Singling out the triangular or kagome layers, possibly via chemical substitution or controlled monolayer growth, may thus lead to systems similar to the ones studied here.

A FQH ground state needs an interaction V that exceeds the bandwidth ($V > W$), but remains smaller than the gap ($V < M$) so that bands are not mixed. Fortunately, TM oxides have substantial Coulomb interactions and NN repulsion V can become as large as or larger than the hoppings. On the other hand, it is almost always smaller than onsite repulsion, which increases one of the two gaps delimiting the flat band [36]. The remaining challenge is thus to keep the effective interaction small compared to the gap separating the bands with $C = \pm 1$. A large figure of merit M/W provides a large window for this separation of energy scales $W < V < M$ and our ED results in Fig. 4 suggest that one indeed has some flexibility in this regard, as interactions differing by a factor of 2 lead to similar results. The crystal-field splitting needed to obtain the desired flattening can be varied by applying (chemical) pressure. Finally, many of these materials, manganites,, in particular, are easy to dope which allows control of the (fractional) band filling.

Theoretically, there is no fundamental objection to the realization of lattice FQH states, but it remains an intriguing challenge from an experimental and practical point of view. We have demonstrated here that d-orbital degrees of freedom, ubiquitous in TM compounds, substantially narrow the topologically nontrivial bands of electrons moving in a background of noncoplanar spins. The separation of energy scales is comparable to that achievable by long-range hopping, and we find signatures of a FQH-like ground state. In the search for the lattice FQH effect, geometrically frustrated TM compounds with an orbital degree of freedom thus come to the fore as a promising class of candidate systems.

This research was supported by the Interphase Program of the Dutch Science Foundation NWO/FOM (J. V. and JvdB) and the Emmy Noether program of the DFG (M. D.) in Germany.

[1] K. v. Klitzing, G. Dorda, and M. Pepper, Phys. Rev. Lett. **45**, 494 (1980).
[2] D. J. Thouless, M. Kohmoto, M. P. Nightingale, and M. den Nijs, Phys. Rev. Lett. **49**, 405 (1982).
[3] F. D. M. Haldane, Phys. Rev. Lett. **61**, 2015 (1988).
[4] C. L. Kane and E. J. Mele, Phys. Rev. Lett. **95**, 146802 (2005).
[5] L. Fu, C. L. Kane, and E. J. Mele, Phys. Rev. Lett. **98**, 106803 (2007).
[6] R. Roy, Phys. Rev. B **79**, 195322 (2009).
[7] J. E. Moore and L. Balents, Phys. Rev. B **75**, 121306 (2007).
[8] B. A. Bernevig, T. L. Hughes, and S.-C. Zhang, Science **314**, 1757 (2006).
[9] M. König, S. Wiedmann, C. Brüne, A. Roth, H. Buhmann, L. W. Molenkamp, X.-L. Qi, and S.-C. Zhang, Science **318**, 766 (2007).
[10] M. Hasan and C. Kane, Rev. Mod. Phys. **82**, 3045 (2010).
[11] X.-L. Qi and S.-C. Zhang, arXiv:1008.2026.
[12] C. Brüne, C. X. Liu, E. G. Novik, E. M. Hankiewicz, H. Buhmann, Y. L. Chen, X. L. Qi, Z. X. Shen, S. C. Zhang, and L. W. Molenkamp, Phys. Rev. Lett. **106**, 126803 (2011).
[13] E. Tang, J.-W. Mei, and X.-G. Wen, Phys. Rev. Lett. **106**, 236802 (2011).
[14] K. Sun, Z. Gu, H. Katsura, and S. D. Sarma, Phys. Rev. Lett. **106**, 236803 (2011).
[15] T. Neupert, L. Santos, C. Chamon, and C. Mudry, Phys. Rev. Lett. **106**, 236804 (2011).
[16] R. B. Laughlin, Phys. Rev. Lett. **50**, 1395 (1983).
[17] X.-L. Qi, arXiv:1105.4298.
[18] S. Das Sarma, M. Freedman, and C. Nayak, Phys. Rev. Lett. **94**, 166802 (2005).
[19] D. N. Sheng, Z.-C. Gu, K. Sun, and L. Sheng, Nature Commun. **2**, 389 (2011).
[20] X. Hu, M. Kargarian, and G. A. Fiete, arXiv:1105.4381.
[21] K. I. Kugel and D. I. Khomskiĭ, Sov. Phys. Usp. **25**, 231 (1982).
[22] Y. Tokura and N. Nagaosa, Science **288**, 462 (2000).
[23] Z. Fang, K. Terakura, and N. Nagaosa, New J. Phys. **7**, 66 (2005).
[24] G. Jackeli and G. Khaliullin, Phys. Rev. Lett. **102**, 017205 (2009).

[25] D. Pesin and L. Balents, Nature Phys. **6**, 376 (2010).
[26] R. Shindou and N. Nagaosa, Phys. Rev. Lett. **87**, 116801 (2001).
[27] I. Martin and C. D. Batista, Phys. Rev. Lett. **101**, 156402 (2008).
[28] Y. Akagi and Y. Motome, J. Phys. Soc. Jpn. **79**, 083711 (2010).
[29] S. Kumar and J. van den Brink, Phys. Rev. Lett. **105**, 216405 (2010).
[30] G.-W. Chern, Phys. Rev. Lett. **105**, 226403 (2010).
[31] K. Ohgushi, S. Murakami, and N. Nagaosa, Phys. Rev. B **62**, R6065 (2000).
[32] Y. Taguchi, Y. Oohara, H. Yoshizawa, N. Nagaosa, and Y. Tokura, Science **291**, 2573 (2001).
[33] X. Chen, S. Dong, and J.-M. Liu, Phys. Rev. B **81**, 064420 (2010).
[34] J. van den Brink, G. Khaliullin, and D. I. Khomskii, Phys. Rev. Lett. **83**, 5118 (1999).
[35] T. Hotta, M. Moraghebi, A. Feiguin, A. Moreo, S. Yunoki, and E. Dagotto, Phys. Rev. Lett. **90**, 247203 (2003).
[36] See Supplemental Material at http://link.aps.org/supplemental/10.1103/PhysRevLett.107.116401 for details and additional figures.
[37] J. C. Slater and G. F. Koster, Phys. Rev. **94**, 1498 (1954); W. A. Harrison, *Electronic Structure and the Properties of Solids* (Dover Publications, New York, 1989). The 90-degree bond angle suppresses hopping via oxygen.
[38] A distortion of the octahedra can induce hopping via the oxygen ligands along some directions, we verified that the total hoppings would have to increase by an unrealistic amount ($\approx 50\%$) before the band flattening is affected.
[39] H. F. Pen, J. van den Brink, D. I. Khomskii, and G. A. Sawatzky, Phys. Rev. Lett. **78**, 1323 (1997).
[40] W. Koshibae and S. Maekawa, Phys. Rev. Lett. **91**, 257003 (2003).
[41] In the $(|xy\rangle, |xz\rangle, |yz\rangle)$ basis, $\{H_{\rm JT}\}_{ij} = -\Delta/3$ for $i \neq j$ and $\{H_{\rm JT}\}_{ii} = 0$.
[42] D. J. Thouless, Phys. Rev. B **40**, 12 034 (1989).
[43] N. Regnault and B. A. Bernevig, arXiv:1105.4867.
[44] Y.-F. Wang, Z.-C. Gu, C.-D. Gong, and D. N. Sheng, arXiv:1103.1686.